# Highspeed multiplexed heterodyne interferometry

**Katharina-S. Isleif,**[1,6] **Oliver Gerberding,**[1,3,4,6] **Sina Köhlenbeck,**[1,6]
**Andrew Sutton,**[2] **Benjamin Sheard,**[1,5] **Stefan Goßler,**[1]
**Daniel Shaddock,**[2] **Gerhard Heinzel,**[1] **and Karsten Danzmann**[1]

[1]*Max-Planck Institute for Gravitational Physics (Albert Einstein Institute), Leibniz University Hannover, Callinstr. 38, 30167 Hannover, Germany*
[2]*Australian National University, Canberra 0200, Australia*
[3]*Now: National Institute of Standards and Technology, Gaithersburg, Maryland 20899, USA*
[4]*Joint Quantum Institute, University of Maryland, College Park, Maryland 20741, USA*
[5]*Now: Kayser-Threde GmbH, Munich, Germany*
[6]*These authors contributed equally to this work*
*katharina-sophie.isleif@aei.mpg.de

**Abstract:** Digitally enhanced heterodyne interferometry is a metrology technique that uses pseudo-random noise codes for modulating the phase of the laser light. Multiple interferometric signals from the same beam path can thereby be isolated based on their propagation delay, allowing one to use advantageous optical layouts in comparison to classic laser interferometers. We present here a high speed version of this technique for measuring multiple targets spatially separated by only a few centimetres. This allows measurements of multiplexed signals using free beams, making the technique attractive for several applications requiring compact optical set-ups like for example space-based interferometers. In an experiment using a modulation and sampling rate of 1.25 GHz we are able to demonstrate multiplexing between targets only separated by 36 cm and we achieve a displacement measurement noise floor of $< 3\,\mathrm{pm}/\sqrt{\mathrm{Hz}}$ at 10 Hz between them. We identify a limiting excess noise at low frequencies which is unique to this technique and is probably caused by the finite bandwidth in our measurement set-up. Utilising an active clock jitter correction scheme we are also able to reduce this noise in a null measurement configuration by one order of magnitude.



**OCIS codes:** (120.0120) Instrumentation, measurement, and metrology; (120.3180) Interferometry; (120.3940) Metrology; (120.4640) Optical instruments; (120.5050) Phase measurement; (120.5060) Phase modulation; (280.4788) Optical sensing and sensors.

## References and links

1. D. A. Shaddock, "Digitally enhanced heterodyne interferometry," Opt. Lett. **32**(22), 3355–3357 (2007).
2. G. de Vine, D. S. Rabeling, B. J. J. Slagmolen, T. T.-Y. Lam, S. Chua, D. M.Wuchenich, D. E. McClelland, and D. A. Shaddock, "Picometer level displacement metrology with digitally enhanced heterodyne interferometry," Opt. Express **17**, 828–837 (2009).
3. D. M. Wuchenich, T. T.-Y. Lam, J. H. Chow, D. E. McClelland, and D. A. Shaddock, "Laser frequency noise immunity in multiplexed displacement sensing," Opt. Lett. **36**(5), 672–674 (2011).
4. T. Kissinger, T. O. H. Charrett, and R. P. Tatam, "Fibre segment interferometry using code-division multiplexed optical signal processing for strain sensing applications," Meas. Sci. Technol. **24**(9), 094011 (2013).

#217101 - $15.00 USD Received 15 Jul 2014; revised 30 Aug 2014; accepted 4 Sep 2014; published 1 Oct 2014

5. A. J. Sutton, O. Gerberding, G. Heinzel, and D. A. Shaddock, "Digitally enhanced homodyne interferometry," Opt. Express **20**, 22195–22207 (2012).
6. K. Danzmann and the LISA study team, "LISA: laser interferometer space antenna for gravitational wave measurements," Classical Quant. Grav. **13**(11A), A247 (1996).
7. P. McNamara, S. Vitale, K. Danzmann, and on behalf of the LISA Pathfinder Science Working Team, "LISA Pathfinder," Classical Quant. Grav. **25**(11), 11403 (2008).
8. B. S. Sheard, G. Heinzel, K. Danzmann, D. A. Shaddock, W. M. Klipstein, and W. M. Folkner, "Intersatellite laser ranging instrument for the GRACE follow-on mission," J. Geod. **86**(12), 1083–1095 (2012).
9. J. Miller, S. Ngo, A. J. Mullavey, B. J. J. Slagmolen, D. A. Shaddock, and D. E. McClelland, "Control and tuning of a suspended Fabry-Perot cavity using digitally enhanced heterodyne interferometry," Opt. Lett. **37**(23), 4952–4954 (2012).
10. D. Shaddock, B. Ware, P. G. Halverson, R. E. Spero, and B. Klipstein, "Overview of the LISA Phasemeter," AIP Conf. Proc. **873**, 654 (2006).
11. O. Gerberding, B. Sheard, I. Bykov, J. Kullmann, J. J. Esteban Delgado, K. Danzmann, and G. Heinzel, "Phasemeter core for intersatellite laser heterodyne interferometry: modelling, simulations and experiments," Classical Quant. Grav. **30**(23), 235029 (2013).
12. O. P. Lay, S. Dubovitsky, D. A. Shaddock, and B. Ware, "Coherent range-gated laser displacement metrology with compact optical head," Opt. Lett. **32**(20), 2933–2935 (2007).
13. J. J. Esteban, A. F. García, J. Eichholz, A. M. Peinado, I. Bykov, G. Heinzel, and K. Danzmann, "Ranging and phase measurement for LISA," J. Phys. Conf. Ser. **228**(1), 012045 (2010).

## 1. Introduction

Optical metrology technologies are used in a wide range of applications. The special case of heterodyne interferometry is a commonly used continuous phase tracking technique that allows measurements with picometre noise over a wide working range. Digitally enhanced heterodyne interferometry combines heterodyne interferometry with optical phase modulation and digital demodulation of pseudo-random noise (PRN) codes [1]. This technique can thereby multiplex optical signals through a single digital measurement chain. The multiplexing capabilities have the potential to make it immune to stray light, they allow common-mode subtraction of several noise sources and they enable to construct interferometers with simpler geometries that share an optical detection path. Previous experiments have already demonstrated that Digital Interferometry (DI) using binary phase-shift keying (BPSK) is capable of measuring with $5\,\mathrm{pm}/\sqrt{\mathrm{Hz}}$ noise at low frequencies [2] and that it can be used to reduce laser frequency noise [3]. It was also shown that a similar scheme can be operated using only a single laser and phase modulation sidebands, leading to a noise floor of $\approx 500\,\mathrm{pm}/\sqrt{\mathrm{Hz}}$ at frequencies around 1 kHz [4]. Additionally, a homodyne variant of DI using quadrature phase-shift keying (QPSK) has also been investigated and achieved performance levels of $\approx 1\,\mathrm{pm}/\sqrt{\mathrm{Hz}}$ above 20 Hz [5].

The most critical parameter of DI, after the displacement sensitivity, is the speed of the PRN modulation and demodulation. It determines the path length difference between multiplexed signals that is necessary for them to be distinguishable. Therefore, increasing the modulation speed is essential to utilise DI in experiments and applications that require compact optical set-ups. This is especially important for space-based missions like LISA (Laser Interferometer Space Antenna) [6], LISA Pathfinder [7] and GRACE Follow-On [8]. Additionally, DI is a candidate technique for performing cavity lock acquisition for future ground based gravitational wave detectors [9] and a higher modulation speed allows to apply it to shorter optical resonators. To this end, we implement a high speed version of DI, using a modulation speed of 1.25 GHz. We analyse the multiplexing capabilities using a free beam set-up and a cavity-like target configuration is used to determine the achievable measurement performance at low frequencies. In addition, we investigate an excess noise source identified to be limiting at low frequencies. This noise has not been present or dominating in earlier experiments with lower modulation speeds and we assume it to be caused by the finite bandwidth of our system. We also present first results on reducing this noise by means of an active clock stabilisation of our digital readout system using a delay-locked loop (DLL).

#217101 - $15.00 USD Received 15 Jul 2014; revised 30 Aug 2014; accepted 4 Sep 2014; published 1 Oct 2014

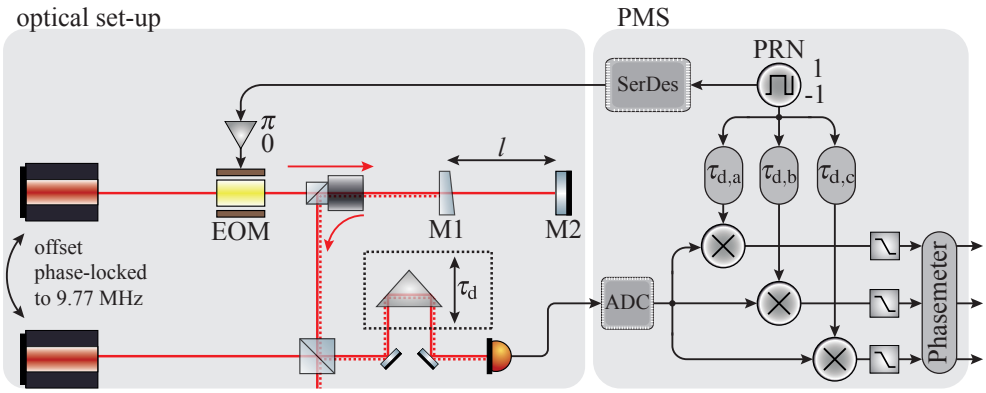


Fig. 1. Simplified schematic of the experimental set-up for digitally enhanced heterodyne interferometry. The optical part is shown on the left. Here, two laser beams with an offset frequency are used to establish the heterodyne interferometer. The phase measurement system (PMS) is shown on the right. It generates the PRN code that is used for the optical phase modulation via an EOM and for the digital demodulation, and it also extracts the phase and amplitude of the digitised and demodulated heterodyne signals.

## 2. Experimental set-up

We construct a heterodyne interferometer (see Fig. 1) with two non-planar ring oscillator (NPRO) lasers operating at 1064 nm. One of them is stabilised to an iodine reference and the other one is phase locked to the first with a frequency offset of 9.77 MHz. In one of the laser beams we introduce a fibre-coupled electro-optical modulator (EOM, NIR-MPX-LN-05 from Photline) with an analogue bandwidth of 7 GHz to generate the PRN phase modulation. The PRN signal itself is generated by a serial transceiver in a field programmable gate array (FPGA) that also contains the phase measurement system (PMS). Before the PRN signal is fed into the EOM it is amplified by a dedicated driver (DR-DG-10-MO from Photline) to achieve a modulation depth of $\pi$. A Faraday rotator, in combination with a polarising beam splitter, is used to spatially separate the modulated light that returns from a two mirror configuration. These mirrors represent the targets of our interferometric measurement and their separation is denoted as $l$. The back-reflections are interfered with the second laser at the recombining beam splitter to generate the readout signal. An additional optical delay line with a translatable corner cube is implemented here to change the overall delay $\tau_\mathrm{d}$ of the interferometric signals. A free beam photo receiver (1567-A from New Focus) with a bandwidth of 12 GHz is used to convert the optical signal into a voltage, preparing it for the PMS.

By means of an analogue-to-digital-converter (ADC), sampling at 1.25 GHz, the photodiode signal is digitised and fed into an FPGA. Here, the signal is split into independent readout channels. In each channel the signal is multiplied with a delayed version $\tau_{\mathrm{d,x}}$ of the PRN code, decimated to 156.25 MHz and then fed into a LISA-style tracking phasemeter, which extracts the phase and amplitude information [10, 11]. The PMS is controlled via a PC and read out with a rate of 36 Hz.

## 3. Multiplexing

DI extracts each signal by correlation against a delayed code, thus the correlation magnitude is related to the return signal power within a specified range gate. To characterise our system we measure the amplitude, and therefore also the correlation, of the decoded signals over a wide

#217101 - $15.00 USD Received 15 Jul 2014; revised 30 Aug 2014; accepted 4 Sep 2014; published 1 Oct 2014

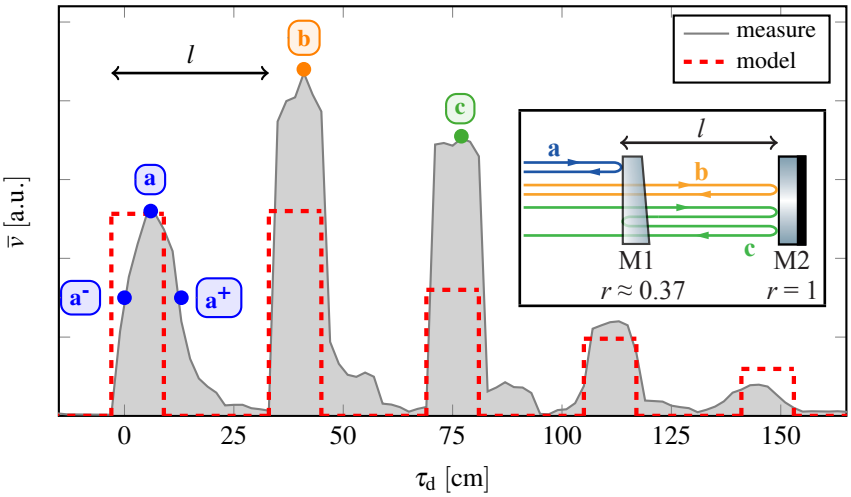


Fig. 2. Measured signal amplitudes of a delay scan using the two-mirror set-up (see inset) with a mirror separation of 36 cm and a PRN rate of 1.25 GHz. The amplitude of the model is determined by the power levels expected from the cavity response for collimated beams. The model also assumes that the bandwidth of the PRN code generation and the signal detection is infinite.

range of demodulation delays. By using the triple mirror delay line we can vary the delay with sub-sample precision (2 cm steps). For the two-mirror constellation with $l = 36$ cm the resulting amplitudes are shown in Fig. 2. The maxima corresponding to the reflection at the first mirror (**a**), the reflection at the second mirror (**b**) and to multiple round trip signals (**c** for the first round trip) are clearly visible. This shows that the system is indeed able to multiplex optical signals with path length differences of only a few centimetres. As expected, by blocking the second mirror all but the first correlation peak vanish (not shown).

However, the measured amplitudes show some significant deviation from ideal values. The first aspect is that the maximum amplitudes of the correlation peaks do not match to the power levels expected from the mirror reflectivities (see red dashed lines in Fig. 2). We do not assume that this is caused by the DI scheme, but rather that the interferometric contrast is not equal for the measured delays. Due to the divergent beam and the non-stable cavity geometry (two planar mirrors) the modes of different back reflections can vary significantly, potentially leading to this effect.

The second deviation to notice is that the form of the peaks is deviating strongly from the ideal rectangular shape expected for an ideal system with infinite bandwidth. Furthermore, the form varies even between the peaks and it sometimes includes additional maxima next to the actual correlation. The slow drop of the correlation from one peak to the next is the reason that we choose a mirror distance of three times our minimal delay separation (3x12 cm), to reduce the inter-signal cross talk.

There are various possible causes for these deformations. To discuss this we remind the reader of the principle behind DI [1]. The PRN code that is phase modulated onto the light can be described by a function $c'(t)$ with values $\{0;\pi\}$. For the demodulation, a delayed copy of the PRN code $c(t-\tau_{d,x})$ is used that has corresponding values $\{1;-1\}$. In the ideal case for a single reflection, the photodiode signal $v_{PD}(t)$ is decoded with the correctly delayed PRN code (see Eq. (1)) and the properties of the phase modulation $c'(t)$ generate a bipolar amplitude modulation (equivalent to BPSK) $c(t)$ (see Eq. (2)). For a fixed delay $\tau_{d,x}$ the amplitude of the

#217101 - $15.00 USD Received 15 Jul 2014; revised 30 Aug 2014; accepted 4 Sep 2014; published 1 Oct 2014

classic heterodyne signal is effectively attenuated by the autocorrelation $c_{\mathrm{corr}}(\tau_{\mathrm{d,x}})$:

$$v = c(t-\tau_{\mathrm{d,x}}) \cdot \underbrace{\overline{v}\sin\left(\omega t + \varphi + c'(t)\right)}_{v_{\mathrm{PD}}(t)} \tag{1}$$

$$= \underbrace{c(t-\tau_{\mathrm{d,x}}) \cdot c(t)}_{c_{\mathrm{corr}}(\tau_{\mathrm{d,x}})} \cdot \underbrace{\overline{v}\sin\left(\omega t + \varphi\right)}_{v_{\mathrm{het}}}. \tag{2}$$

In the experimental set-up some of these assumptions are not perfectly met. While the demodulation, which is performed inside the PMS, is perfect, the modulation $c'(t)$ is not. The non-rectangular modulation signal from the serial transceiver and the bandwidth limitations of the cables, the amplifier and the EOM itself can significantly deform $c'(t)$. Similarly, the transfer functions of the photodiode and the ADC will reshape the modulated heterodyne signal $v_{\mathrm{PD}}(t)$. A combination of these effects is assumed to be responsible for the measured amplitude shown in Fig. 2. Most components in the experiment have a sufficiently wide bandwidth ($> 5\,\mathrm{GHz}$), only the transfer function of the ADC front-end is not well known and it is believed to be the limiting factor. Bandwidth limitations alone do, however, not explain the shape differences between the peaks and, therefore, a full understanding is not yet available. We believe that the use of GHz modulations and the accompanying issues related to cross-talk, impedance matching and drive signal amplification are at least partly responsible for these deviations.

## 4. Displacement measurement performance

We investigate the performance, i.e. the displacement sensitivity and linearity, of the phase readout from the multiplexed signals using the two-mirror constellation (see inset of Fig. 2). The relative motion $\tilde{l}$ between M1 and M2 is encoded in the phase difference between reflections **a** and **b**:

$$\tilde{l}_{\mathrm{ba}} = \frac{2\pi}{\lambda}(\varphi_{\mathrm{b}} - \varphi_{\mathrm{a}}) =: \frac{2\pi}{\lambda}\varphi_{\mathrm{ba}}. \tag{3}$$

The same motion is also measured with the phase difference between signals **a** and **c**:

$$\tilde{l}_{\mathrm{ca}} = \frac{2\pi}{\lambda}(\varphi_{\mathrm{c}} - \varphi_{\mathrm{a}})/2 =: \frac{2\pi}{\lambda}\varphi_{\mathrm{ca}}/2. \tag{4}$$

Both of these combinations, as well as the directly measured phases, have been tracked over a long time to determine the performance at low frequencies. The results are shown as displacement spectral densities in Fig. 3. We find a significant rejection of common-mode noise, as expected for DI, between the directly measured phases $\tilde{l}_x$ (blue) and the signal combinations that correspond to the relative mirror motion (orange, green). The performance of this displacement measurement is limited by thermal and acoustic effects since we are not operating in vacuum. To determine the actual limitations of the DI readout scheme we subtract the two signal combinations to perform a null measurement:

$$\Delta\tilde{l} = \tilde{l}_{\mathrm{ba}} - \tilde{l}_{\mathrm{ca}} \approx 0. \tag{5}$$

The resulting noise floor is the red line in Fig. 3. In addition to an expected white noise floor, caused either by electronic noise or the PRN modulation itself [12], we observe a performance decrease to lower frequencies. However, we do achieve a level of $3\,\mathrm{pm}/\sqrt{\mathrm{Hz}}$ at 10 Hz and $1\,\mathrm{nm}/\sqrt{\mathrm{Hz}}$ at 1 mHz, which is already sufficient for applications for satellite geodesy missions [8]. The achieved dynamic range is at least 4 orders of magnitude at 10 mHz for the measurement shown in Fig. 3.

To investigate the unknown noise and to exclude optical effects and cross talk between **a**, **b** and **c**, we perform measurements using an alternative zero combination. By tuning the overall

#217101 - $15.00 USD Received 15 Jul 2014; revised 30 Aug 2014; accepted 4 Sep 2014; published 1 Oct 2014

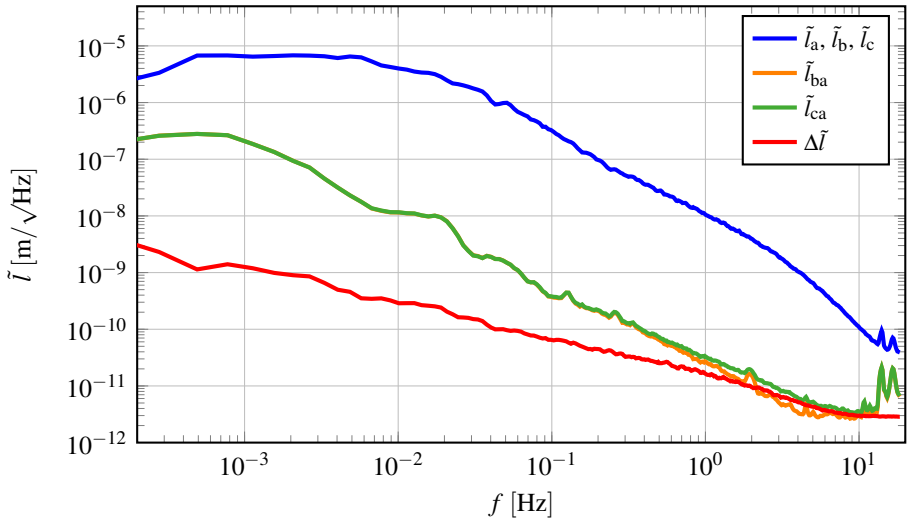


Fig. 3. Displacement spectral density of the two-mirror set-up using a phase modulation of 1.25 GHz and a mirror separation of 36 cm. Shown is the phase noise of the initial signals $\tilde{l}_x$ (blue), the relative mirror motions $\tilde{l}_{ba}$ (orange) and $\tilde{l}_{ca}$ (green) and the null measurement $\Delta\tilde{l}$ (red).

delay we read out the phase of only the first reflection using two consecutive PRN delays ($\mathbf{a^-}, \mathbf{a^+}$ in Fig. 2), while blocking the second mirror. Both of these signals contain the exact same optical path length, therefore their phase difference should combine to zero:

$$\tilde{\varepsilon} = \frac{2\pi}{\lambda}(\varphi_{a^+} - \varphi_{a^-}) \approx 0. \tag{6}$$

The results of this measurement with a PRN rate of 1.25 GHz are shown in Fig. 4 (green). We find an excess noise increasing to low frequencies, which is likely the same one observed in the two-mirror measurements.

To exclude the presence of classic heterodyne interferometer noise sources in the zero combinations we analysed the coupling of laser frequency and amplitude noise and found both to be negligible. By using different PRN repetition lengths we confirmed that these do not influence the noise at low frequencies as would be indicative of higher or lower PRN autocorrelation with a change in code length. We therefore conclude that the effect must be unique to the DI scheme.

## 5. Clock noise coupling due to limited bandwidth

If we assume the PRN correlation does only influence the signal amplitudes (see Eqs. (1) and (2)), one would not expect the phase noise present in $\tilde{\varepsilon}$. However, since the bandwidth of our system is limited, a coupling between the delay, which determines the correlation, and the measured phase might exist. If such a coupling is present, any variations in the overall delay $\tau_d$ would create a phase change and the coupling factor would depend on the delay position on the correlation peak. Such a delay can easily be introduced by clock noise in either the transmission or detection of the modulated signals.

Based on this assumption, we introduce the possibility to modulate the clock of the serial transceiver relative to the ADC clock in our experiment. Thereby, we can directly influence $\tau_d$. By applying a low frequency modulation to this clock we find a significant coupling into $\tilde{\varepsilon}$, both in the signal phases and amplitudes. The coupling is found to be on the order of 100 pm

#217101 - $15.00 USD Received 15 Jul 2014; revised 30 Aug 2014; accepted 4 Sep 2014; published 1 Oct 2014

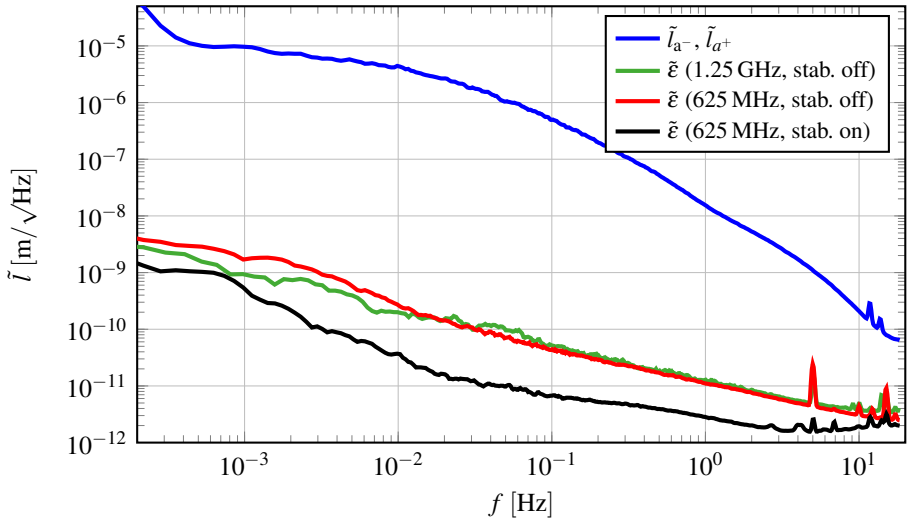


Fig. 4. Displacement spectral density of the single-mirror set-up sampled with 1.25 GHz and with and without active clock stabilisation. Shown is the displacement noise of the initial signals $\tilde{l}_x$ (blue) by using a PRN modulation rate of 1.25 GHz and without DLL, the corresponding null measurement $\tilde{\varepsilon}$ is shown in the second plot (green). A reduction of the modulation rate to 625 MHz shows likely the same displacement noise $\tilde{l}_x$ (blue) and a similar $\tilde{\varepsilon}$ (red). The achieved performance for $\tilde{\varepsilon}$, by applying the clock stabilisation, is given by the final plot (black).

displacement noise for a clock modulation amplitude of 1 ps. Since the overall delay also includes the optical path length of the beams, it is also useful to determine the coupling factor of actual length changes into the displacement measurement. Transferring the 1 ps into a length in vacuum this corresponds to $\approx 3$ mm, giving a coupling of 1 pm/30 µm.

To validate that this effect is indeed limiting our measurements we implement an additional active clock stabilisation. We reduce the modulation rate to 625 MHz such that we can use the amplitude difference of $\mathbf{a^-}$ and $\mathbf{a^+}$ (now separated by an additional demodulation delay) as correlation detector. Combined with a servo controller and a feedback to the clock modulation input we create a delay-locked loop (DLL) [13], that actively keeps $\tau_\mathrm{d}$ constant. In Fig. 4 we show $\tilde{\varepsilon}$ with (black) and without (red) this stabilisation. The DLL improves the performance of this measurement significantly, one order of magnitude in noise reduction is achieved between a few mHz and 1 Hz. The use of the DLL in the two mirror set-up shows no improvements and this might partly be caused by the length to length coupling described in the previous paragraph.

A reduction of the PRN modulation rate should, if the analogue system bandwidth is indeed the cause of the delay dependent phase, also improve the system performance. However, as shown in Fig. 4, no significant changes are visible between the unstabilised measurements at 1.25 GHz and 625 MHz. It remains to be investigated if the even lower modulation rates used in other implementations of DI [2] caused the clock induced phase noise to be non-limiting at low frequencies.

## 6. Conclusion and outlook

This article reports on the implementation of a high speed digitally enhanced heterodyne interferometer using off-the-shelf components. Optical measurements using PRN modulation rates of 1.25 GHz with targets separated by only 36 cm, show performance levels of 3 pm/$\sqrt{\text{Hz}}$ at

#217101 - $15.00 USD Received 15 Jul 2014; revised 30 Aug 2014; accepted 4 Sep 2014; published 1 Oct 2014

10 Hz and 1 nm/$\sqrt{\text{Hz}}$ at 1 mHz. A coupling of clock noise into the phase measurement is present and limits the performance in a single reflection zero measurement. An active clock stabilisation via a delay-locked loop allows one to reduce this noise by an order of magnitude at low frequencies.

Future, even faster implementations of this scheme might benefit from dedicated hardware that has less clock jitter between PRN code generation and ADC. A comprehensive analytic or numeric model of the effects of non-ideal modulations and bandwidth limitations will also give a better understanding of the parameters that influence the achievable low frequency performance.

#217101 - $15.00 USD Received 15 Jul 2014; revised 30 Aug 2014; accepted 4 Sep 2014; published 1 Oct 2014